Influence of Delayed Conductance on Neuronal Synchronization

Paulo R. Protachevicz [1,2], Fernando S. Borges [3], Kelly C. Iarosz [1,4,5*], Murilo S. Baptista [6], Ewandson L. Lameu [7], Matheus Hansen [2,8], Iberê L. Caldas [1], José D. Szezech Jr. [2,8], Antonio M. Batista [1,2,8] and Jürgen Kurths [9,10,11]

[1] Instituto de Física, Universidade de São Paulo, São Paulo, Brazil, [2] Graduate Program in Science–Physics, State University of Ponta Grossa, Ponta Grossa, Brazil, [3] Center for Mathematics, Computation, and Cognition, Federal University of ABC, São Paulo, Brazil, [4] Faculdade de Telêmaco Borba, FATEB, Telêmaco Borba, Brazil, [5] Graduate Program in Chemical Engineering, Federal Technological University of Paraná, Ponta Grossa, Brazil, [6] Institute for Complex Systems and Mathematical Biology, SUPA, University of Aberdeen, Aberdeen, United Kingdom, [7] Cell Biology and Anatomy Department, University of Calgary, Calgary, AB, Canada, [8] Department of Mathematics and Statistics, State University of Ponta Grossa, Ponta Grossa, Brazil, [9] Department of Physics, Humboldt University, Berlin, Germany, [10] Department Complexity Science, Potsdam Institute for Climate Impact Research, Potsdam, Germany, [11] Department of Human and Animal Physiology, Saratov State University, Saratov, Russia

In the brain, the excitation-inhibition balance prevents abnormal synchronous behavior. However, known synaptic conductance intensity can be insufficient to account for the undesired synchronization. Due to this fact, we consider time delay in excitatory and inhibitory conductances and study its effect on the neuronal synchronization. In this work, we build a neuronal network composed of adaptive integrate-and-fire neurons coupled by means of delayed conductances. We observe that the time delay in the excitatory and inhibitory conductivities can alter both the state of the collective behavior (synchronous or desynchronous) and its type (spike or burst). For the weak coupling regime, we find that synchronization appears associated with neurons behaving with extremes highest and lowest mean firing frequency, in contrast to when desynchronization is present when neurons do not exhibit extreme values for the firing frequency. Synchronization can also be characterized by neurons presenting either the highest or the lowest levels in the mean synaptic current. For the strong coupling, synchronous burst activities can occur for delays in the inhibitory conductivity. For approximately equal-length delays in the excitatory and inhibitory conductances, desynchronous spikes activities are identified for both weak and strong coupling regimes. Therefore, our results show that not only the conductance intensity, but also short delays in the inhibitory conductance are relevant to avoid abnormal neuronal synchronization.

Keywords: synchronization, integrate-and-fire, neuronal network, time delay, conductance

1. INTRODUCTION

Network physiology reveals how organ systems dynamically interact (Bartsch et al., 2015). The human organism is a complex physiological and integrated system in which a fail in a specific component can produce a range of biological effects (Bashan et al., 2012). One of the biggest challenges is to understand how global behavior of the human organism emerges due to local causes (Ivanov et al., 2016). Brain-brain and brain-organ networks have been considered to study integrated physiological systems under neuronal control (Ivanov et al., 2009). Chen et al. (2006)

investigated the relationship between the blood flow velocities in the cerebral arteries and beat-to-beat blood pressure. Liu et al. (2015) built a network of brain wave interactions. They found complex brain dynamics, such as desynchronous and synchronous activities (Xu et al., 2006) during quiet wake and deep sleep, respectively.

Time delay has been considered in several problems of biological interest (Glass et al., 1988), such as herbivore dynamics (Sun et al., 2015), polymerization processes (Mier-y-Terán-Romero et al., 2010), dynamics of tumor growth (Byrne, 1997; Borges et al., 2014), and dynamic behavior of coupled neurons (Esfahani et al., 2016). One of the brain's intrinsic properties is the delay in the transmission of information among separate brain regions (Deco et al., 2009). Stoelzel et al. (2017) investigated the relation between axonal conduction delays and visual information. They found that some conduction times in corticothalamic axons exceed 50 ms. Conduction latencies in mammalian brain about 100 ms are also reported by Aston-Jones et al. (1985).

Dynamic brain behavior can be mimicked by means of neuronal network models (Protachevicz et al., 2019), for instance, neuronal synchronous behavior (Borges et al., 2018). Neuronal synchronization is found in task conditions (Deco et al., 2011). Furthermore, many neurological disorders are also related to synchronous behavior in the brain (Uhlhaas and Singer, 2006). Network models have been used to study the effects of time delay in synchronized neuronal activities (Stepan, 2009). Dhamala et al. (2004) showed the enhancement of neuronal synchrony by time delay in a neuronal network. Wang et al. (2016) investigated synchronized stability in coupled neurons with distributed and discrete delays. Kim and Lim (2018a,b) studied synchronization in networks, where they considered plasticity (Borges et al., 2017a) and time delays between the pre-synaptic and post-synaptic spike times.

Neurons can be modeled by differential equations. In 1907, Lapicque (Lapicque, 1907) used a linear differential equation (leaky integrate-and-fire) to simulate the neuron membrane potential. A system of non-linear differential equations was proposed by Hodgkin and Huxley (1952) to describe the action potential. The Hodgkin-Huxley model considers ion channels that open and close according to the voltage. Different connectivities among the neurons have been considered to form neuronal networks. The dynamics of coupled neurons was investigated in networks with random connections (Brunel, 2000), small-world (Tang et al., 2011), and scale-free (Batista et al., 2007, 2010) topologies were used to study neuronal synchronization.

We build here a network composed of adaptive exponential integrate-and-fire (AEIF) neurons. The AEIF model was introduced by Brette and Gerstner (2005). Depending on the parameter values, the AEIF neuron can exhibit different firing patterns (Naud et al., 2008). Synchronized firing patterns were observed in coupled AEIF neurons (Borges et al., 2017b). Pérez et al. (2011) studied the influence of conduction delays on spike synchronization in Hodgkin-Huxley neuronal networks. Previous works found that slow-rising inhibitory synaptic currents can induce synchrony (Abbott and van Vreeswijk,

1993; van Vreeswijk et al., 1994) and affect the stability of asynchronous state (e.g., splay state) (van Vreeswijk, 1996; Olmi et al., 2014). Chen et al. (2017) reported that the competition between coupling strength and synaptic time-constant leads to rich bifurcation in pulse-coupled neuronal networks with either excitatory or inhibitory synapses.

In this work, we study AEIF neurons randomly connected by means of excitatory and inhibitory conductivities. The neurons can exhibit not only spike but also burst activities (Santos et al., 2019). Our results show that the delayed conductance in both excitatory and inhibitory connections play an important role in the neuronal synchronization. Furthermore, we demonstrate that not only the values of the conductance intensity, but also small delays in inhibitory conductances are important to prevent abnormal synchronization.

The paper is organized as follows. In section 2, we introduce the neuronal network composed of AEIF neurons and delayed conductance. Section 3 shows our results about the effects of conduction delays in neuronal synchronization. We draw our conclusions in the last section.

2. MODEL AND METHODS

We construct a neuronal network with 100 AEIF neurons, where the connections are randomly chosen with probability equal to 0.5. The connection probability is defined as

$$p = \frac{N_T}{N \cdot (N-1)}, \tag{1}$$

where N_T is the total connection number of the network and $N \cdot (N-1)$ is the maximal possible number of connections for a

TABLE 1 | Standard parameter set.

Parameter	Description	Value
N	Number of AEIF on the network	100 neurons
C	Capacitance membrane	200 pF
g_L	Leak conductance	12 nS
E_L	Resting potential	−70 mV
I_i	Constant input current	$2 \cdot I_{rheo}$
Δ_T	Slope factor	2 mV
V_T	Potential threshold	−50 mV
τ_w	Adaptation time constant	300 ms
a_i	Level of subthreshold adaptation	[1.9, 2.1] nS
b	Level of triggered adaptation	70 pA
V_r	Reset potential	−58 mV
V_{REV}^{exc}	Excitatory synaptic reversal potential	0 mV
V_{REV}^{inh}	Inhibitory synaptic reversal potential	−80 mV
A_{ij}	Adjacent matrix elements	0 or 1
τ_s	Synaptic time constant	2.728 ms
t_{fin}	Final time to analyses	10 s
t_{ini}	Initial time to analyses	5 s
g_s	Chemical conductance	g_{exc} or g_{inh}
d_j	Time delay	d_{exc} or d_{inh}

network with N neurons without auto-connections. We consider that each neuron has at least one connection. The network has 80 and 20% of excitatory and inhibitory connections, respectively (Noback et al., 2005). The network dynamics is given by

$$C\frac{dV_i}{dt} = -g_L\left(V_i - E_L\right) + g_L\Delta_T\exp\left(\frac{V_i - V_T}{\Delta_T}\right)$$
$$-w_i + I_i + I_i^{syn}, \tag{2}$$

$$\tau_w\frac{dw_i}{dt} = a_i\left(V_i - E_L\right) - w_i, \tag{3}$$

$$\tau_s\frac{dg_i}{dt} = -g_i, \tag{4}$$

where V_i, w_i, and g_i are the membrane potential, the adaptation current, and the conductance of the neuron i, respectively. We consider $C = 200$ pF (capacitance membrane), $g_L = 12$ nS (leak conductance), $E_L = -70$ mV (resting potential), $I_i = 2 \cdot I_{\text{rheo}}$ (constant input equal to two times the rheobase current Naud et al., 2008), $\Delta_T = 2$ mV (slope factor), $V_T = -50$ mV (potential threshold), and $\tau_w = 300$ ms (adaptation time constant). The level of subthreshold adaptation a_i is randomly distributed in the interval $[1.9, 2.1]$ nS. This set of parameters corresponds to the spike adaptation activity when neurons are uncoupled. In the model, the adaptation mechanism is able to generate burst activities when the neurons are connected by excitatory synapses (Fardet et al., 2018). For weak coupling, the neurons exhibit spike activities, while for strong, burst activities can occur for low inhibition (Protachevicz et al., 2019). The current input I_i^{syn} is calculated by the expression
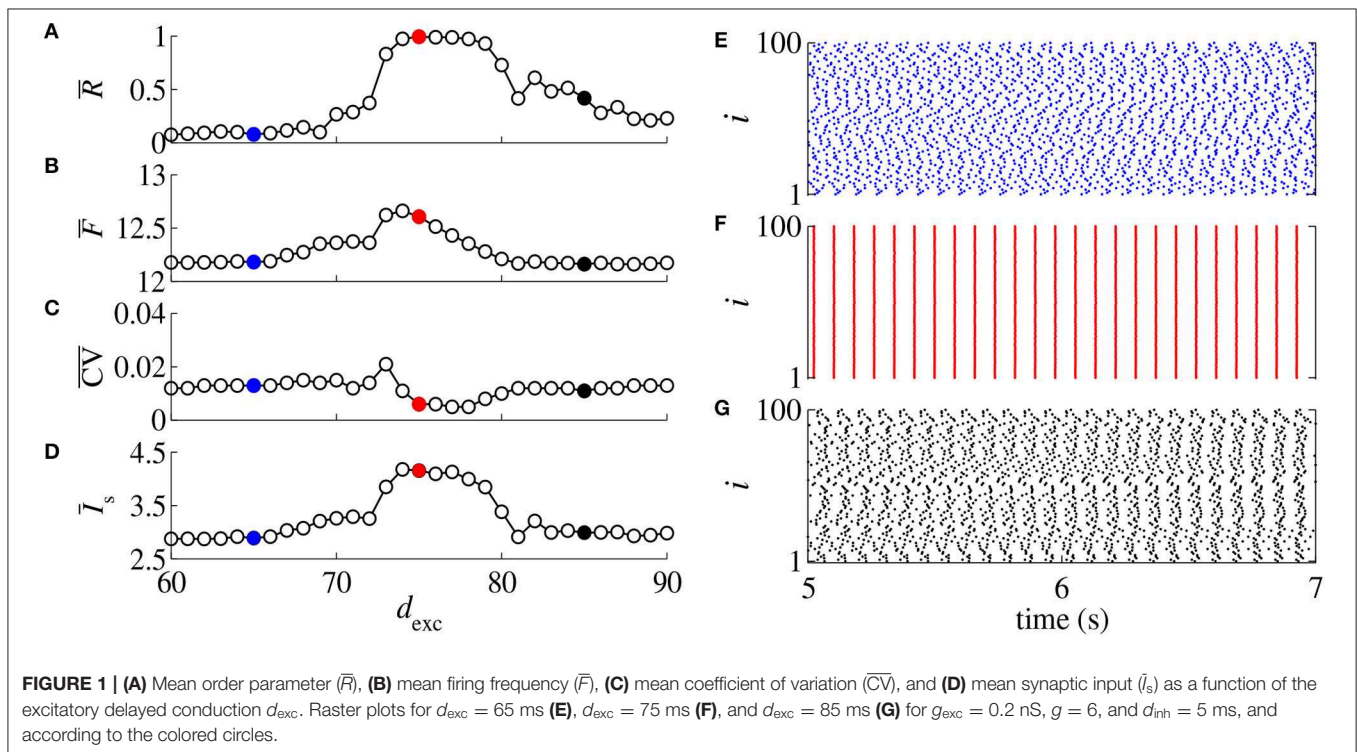
$$I_i^{syn}(t) = \sum_{j=1}^{N}\left[V_{REV}^j - V_i(t)\right]A_{ij}g_j(t - d_j), \tag{5}$$

where d_j is the time delay in the conductance. We consider $d_j = d_{\text{inh}}$ for inhibitory and $d_j = d_{\text{exc}}$ for excitatory neurons. V_{REV}^j is the reversal potential ($V_{REV} = 0$ mV for excitatory and $V_{REV} = -80$ mV for inhibitory synapses). In the adjacency matrix (A_{ij}), the element value is equal to 1 when the presynaptic neuron j and post-synaptic neuron i are connected, and 0 when they are not connected. g_j has an exponential decay with the synaptic time constant $\tau_s = 2.728$ ms. When the membrane potential of the neuron i is above a threshold ($V_i > V_{\text{thres}}$) (Naud et al., 2008), the state variables are updated according to the rules

$$V_i \rightarrow V_r,$$
$$w_i \rightarrow w_i + b, \tag{6}$$
$$g_i \rightarrow g_i + g_s,$$

where $V_r = -58$ mV is the reset potential and $b = 70$ pA is the triggered adaptation addition. The chemical conductance g_s assumes g_{exc} and g_{inh} for excitatory and inhibitory neurons, respectively. We define a relative inhibitory conductance as $g = g_{\text{inh}}/g_{\text{exc}}$. **Table 1** shows the standard parameter set that we use in our simulations.

As a diagnostic tool to identify synchronization, we use the time average of the Kuramoto order parameter (Kuramoto, 1984; Batista et al., 2017)

FIGURE 1 | (A) Mean order parameter ($\overline{R}$), **(B)** mean firing frequency ($\overline{F}$), **(C)** mean coefficient of variation ($\overline{CV}$), and **(D)** mean synaptic input ($\overline{I}_s$) as a function of the excitatory delayed conduction d_{exc}. Raster plots for $d_{\text{exc}} = 65$ ms **(E)**, $d_{\text{exc}} = 75$ ms **(F)**, and $d_{\text{exc}} = 85$ ms **(G)** for $g_{\text{exc}} = 0.2$ nS, $g = 6$, and $d_{\text{inh}} = 5$ ms, and according to the colored circles.

$$\overline{R} = \frac{1}{t_{\text{fin}} - t_{\text{ini}}} \int_{t_{\text{ini}}}^{t_{\text{fin}}} \left| \frac{1}{N} \sum_{j=1}^{N} \exp(i\Phi_j(t)) \right| dt, \qquad (7)$$

where the final time in the simulation and initial time for analyses are $t_{\text{fin}} = 10$ s and $t_{\text{ini}} = 5$ s, respectively. $\overline{R}$ ranges from 0 to 1 and approaches 1 for synchronous behavior. The phase of each neuron j is calculated by Pikovsky et al. (1997)

$$\Phi_j(t) = 2\pi m + 2\pi \frac{t - t_{j,m}}{t_{j,m+1} - t_{j,m}}, \qquad (8)$$

where $t_{j,m}$ is the time at which neuron j suffers its m-th spike ($m = 0, 1, 2, \dots$) and Φ is defined between two spikes in the interval $[t_{j,m}, t_{j,m+1}]$.

The AEIF neuron can exhibit spike or burst activities. To identify these activities, we compute the coefficient of variation of the inter-spike interval (ISI)

$$\overline{CV} = \frac{\sigma_{\text{ISI}}}{\overline{\text{ISI}}}, \qquad (9)$$

where σ_{ISI} and $\overline{\text{ISI}}$ are the standard deviation and the mean value of ISI, respectively. We identify spike activities when $\overline{CV} < 0.5$ and burst activities when $\overline{CV} \geq 0.5$ (Protachevicz et al., 2018).
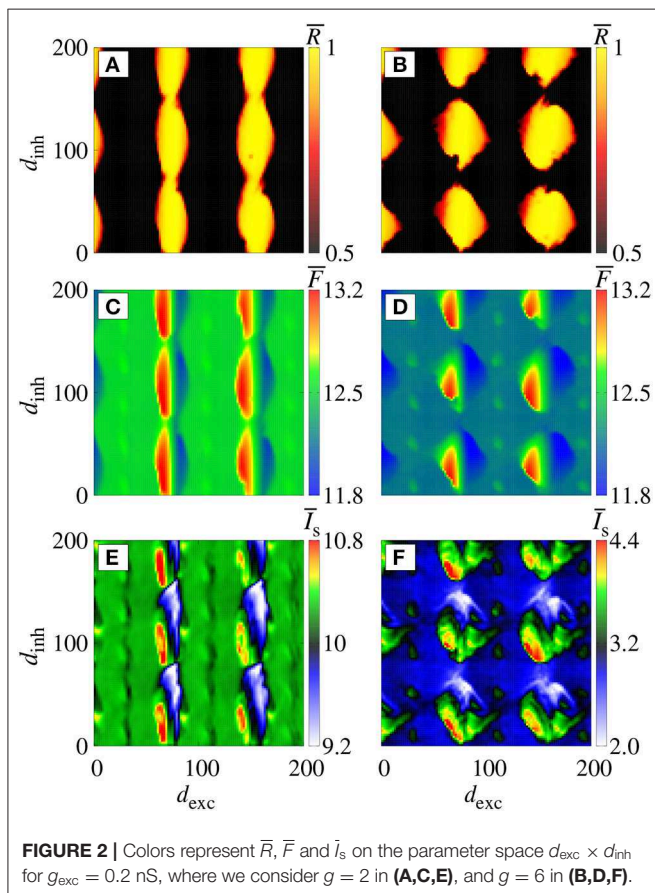
We calculate the mean firing frequency $\overline{F}$(Hz) of the neuronal network by mean of the expression
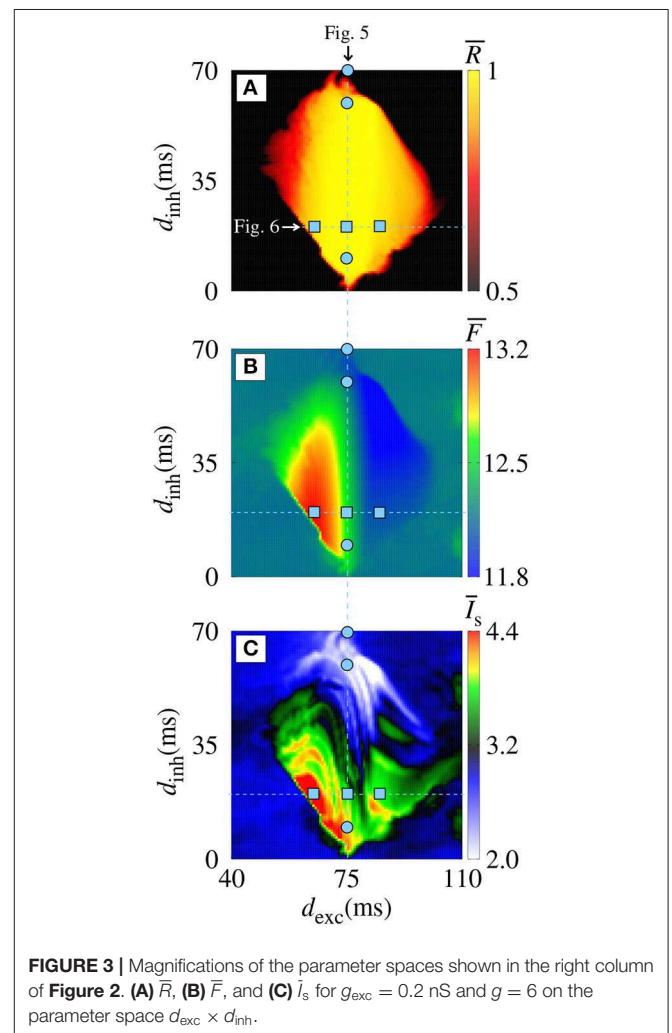
$$\overline{F} = \frac{1}{\overline{\text{ISI}}}. \qquad (10)$$

We also compute the instantaneous $I^{\text{syn}}(t)$ and the mean synaptic input $\bar{I}_s$ (pA) of the network through

$$I^{\text{syn}}(t) = \frac{1}{N} \sum_{i=1}^{N} I_i^{\text{syn}}(t), \qquad (11)$$

$$\bar{I}_s = \frac{1}{(t_{\text{fin}} - t_{\text{ini}})} \int_{t_{\text{ini}}}^{t_{\text{fin}}} I^{\text{syn}}(t) dt, \qquad (12)$$

where $I_i^{\text{syn}}(t)$ is described by Equation (5). In all diagnostics, each point in the parameter space $d_{\text{inh}} \times d_{\text{exc}}$ is computed by means of the average of 10 different initial conditions. The initial conditions of V_i and w_i are randomly distributed in the interval $V_i = [-70, -50]$ mV and $w_i = [0, 80]$ nA, respectively. The

FIGURE 2 | Colors represent $\overline{R}$, $\overline{F}$ and $\bar{I}_s$ on the parameter space $d_{\text{exc}} \times d_{\text{inh}}$ for $g_{\text{exc}} = 0.2$ nS, where we consider $g = 2$ in (A,C,E), and $g = 6$ in (B,D,F).

FIGURE 3 | Magnifications of the parameter spaces shown in the right column of Figure 2. (A) $\overline{R}$, (B) $\overline{F}$, and (C) $\bar{I}_s$ for $g_{\text{exc}} = 0.2$ nS and $g = 6$ on the parameter space $d_{\text{exc}} \times d_{\text{inh}}$.
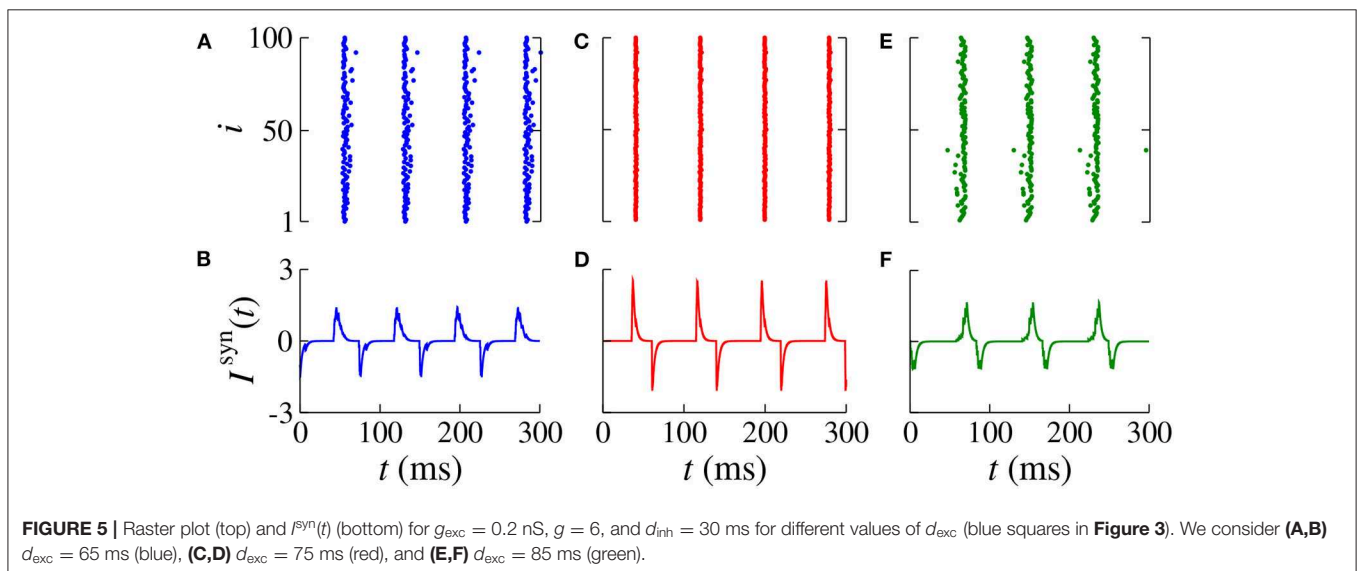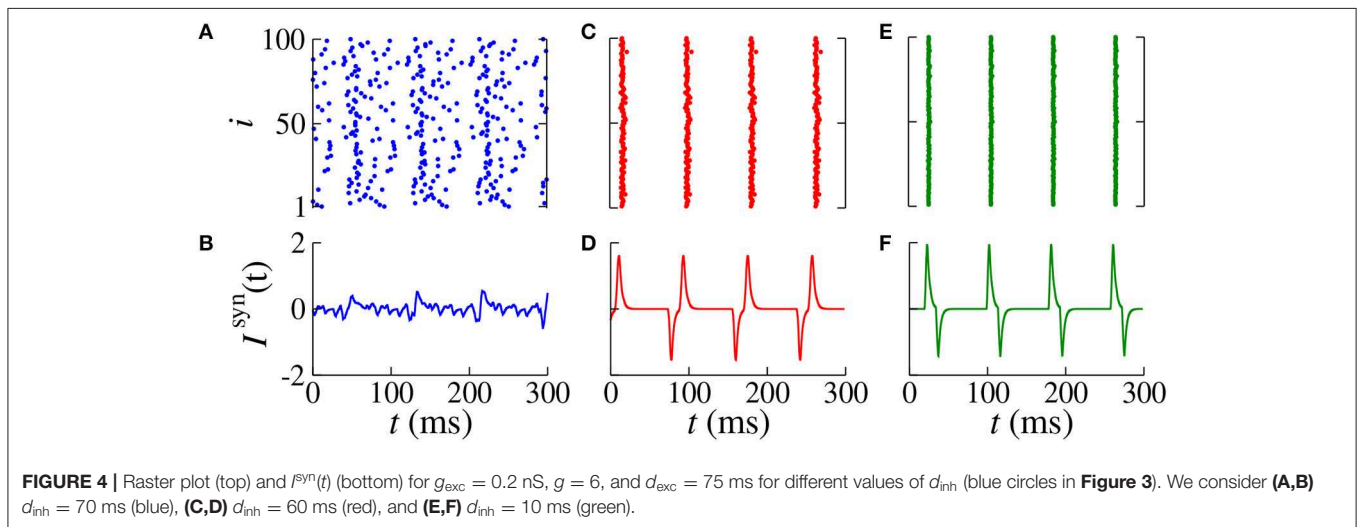
initial conductance g_i is equal to 0 for all neurons. To solve the delayed differential equations, we consider an initial profile of the network (for $t \in [-d_j, 0]$) in which the neurons are not spiking.

3. RESULTS

Neuronal conductances play a key role in network responses to stimuli (di Volo et al., 2019). Conduction delays were observed between the activities of the pre-synaptic and post-synaptic neurons (Ermentrout and Kopell, 1998). **Figures 1A–D** display $\overline{R}$, $\overline{F}$, $\overline{CV}$, and $\overline{I}_s$, respectively, as a function of d_{exc} for $g_{exc} = 0.2$ nS, $g = 6$, and $d_{inh} = 5$ ms. In **Figures 1E–G** (blue points, red points, black points), we show the raster plots for the parameters indicated by the respective filled colored circles. In **Figures 1A–D**, increasing d_{exc} from 65 ms (blue) to 75 ms (red), the desynchronized spikes (**Figure 1E**) go to a synchronous behavior (**Figure 1F**), however, the spikes desynchronize when

d_{exc} is increased to 85 ms (**Figure 1G**). We find that a small change of the delayed conductance value can improve or suppress synchronous behavior.

Figures 2A,B display the parameter space $d_{inh} \times d_{exc}$ for $g_{exc} = 0.2$ nS (weak coupling), where the color bar corresponds to the average order parameter $\overline{R}$. The parameter space exhibits synchronous (yellow region) and desynchronous (black region) spike patterns ($\overline{CV} < 0.5$). For $g = 2$ (**Figure 2A**), we verify vertical domains of synchronization that can be reached by maintaining d_{inh} constant, and varying d_{exc}. Increasing the relative inhibitory conductance for $g = 6$, separated domains with synchronized spikes appear, as shown in **Figure 2B**. For the considered parameter space, the highest and lowest values of $\overline{F}$ (**Figures 2C,D**) and $\overline{I}_s$ (**Figures 2E,F**) appear in the synchronized domain. In the domains with synchronized activities, we observe that the neuronal network achieves and maintains synchronized activities by means of changes in the mean firing frequency and synaptic current. In the region

FIGURE 4 | Raster plot (top) and $I^{syn}(t)$ (bottom) for $g_{exc} = 0.2$ nS, $g = 6$, and $d_{exc} = 75$ ms for different values of d_{inh} (blue circles in **Figure 3**). We consider **(A,B)** $d_{inh} = 70$ ms (blue), **(C,D)** $d_{inh} = 60$ ms (red), and **(E,F)** $d_{inh} = 10$ ms (green).

FIGURE 5 | Raster plot (top) and $I^{syn}(t)$ (bottom) for $g_{exc} = 0.2$ nS, $g = 6$, and $d_{inh} = 30$ ms for different values of d_{exc} (blue squares in **Figure 3**). We consider **(A,B)** $d_{exc} = 65$ ms (blue), **(C,D)** $d_{exc} = 75$ ms (red), and **(E,F)** $d_{exc} = 85$ ms (green).

with a desynchronous pattern, the excitatory and inhibitory synaptic currents arrive in the neurons approximately at the same time.

Figure 3 displays magnifications of the parameter spaces shown in the right column of **Figure 2** ($40 \leq d_{exc} \leq 110$ ms and $0 \leq d_{inh} \leq 70$ ms). In the domain with a synchronous pattern, we observe that d_{exc} and d_{inh} have a significant influence on the mean firing frequency and mean synaptic current, respectively. The dynamics of neurons for some values of d_{exc}, indicated in the vertical line (blue circles) in **Figure 3** for $d_{exc} = 75$ ms, are shown in **Figure 4** by means of the temporal evolution of i (A,C,E) and I^{syn} (B,D,F), where we consider $d_{inh} = 70$ ms (blue), $d_{inh} = 60$ ms (red), and $d_{inh} = 10$ ms (green).

In **Figures 4A,B**, we verify the existence of desynchronous spikes when excitatory and inhibitory inputs arrive in almost the same time ($d_{exc} \approx d_{inh}$). **Figure 5** shows raster plots (top) and $I^{syn}(t)$ (bottom) for $d_{inh} = 30$ ms (blue squares in **Figure 3**), where we consider $d_{exc} = 65$ ms (blue), $d_{exc} = 75$ ms (red), and $d_{exc} = 85$ ms (green). The parameters correspond to the region where synchronization can occur. Furthermore, we observe that depending on the excitatory delay value, synchronization can be improved. We verify that the synchronization is improved for $d_{exc} = 75$ ms, namely certain values of the delay can optimize the synchronization regime.

Increasing g_{exc} from 0.2 to 0.8 nS (strong coupling), in **Figure 6**, we observe in another range of the parameter space $d_{inh} \times d_{exc}$ (**Figure 6A**) where the region with synchronous behavior increases. **Figure 6B** displays the existence of regions with spike (blue) and burst (red) through the coefficient of variation value. Comparing **Figures 6A,B**, we verify that there are not only synchronized spikes, but also synchronized bursts. Moreover, desynchronous spike patterns are found for $d_{inh} \approx d_{exc}$. **Figures 6C,D** show in color scale the values of $\overline{F}$ and $\overline{I}_s$, respectively. We see that the synchronized spikes occur for the values of d_{inh} and d_{exc} in which $\overline{F}$ and $\overline{I}_s$ are low. The synchronized bursts can be found with different values of $\overline{F}$ and $\overline{I}_s$. In addition, we also observe desynchronized activities for $d_{inh} \approx d_{exc}$. **Figure 7** displays the raster plot (top) and $I^{syn}(t)$ (bottom) for $g_{exc} = 0.8$ nS, $g = 6$, and different values of d_{exc} and d_{inh}, according to the parameters pointed by the symbols in **Figure 6**. Different delay values can generate desynchronized spikes (**Figures 7A,B**), synchronized bursts (**Figures 7C,D,G,H**), and synchronized spikes (**Figures 7E,F**).

FIGURE 6 | **(A)** $\overline{R}$, **(B)** $\overline{CV}$, **(C)** $\overline{F}$, and **(D)** $\overline{I}_s$ in the parameter space $d_{exc} \times d_{inh}$ for $g_{exc} = 0.8$ nS and $g = 6$. Symbols in $d_{exc} \times d_{inh}$ correspond to $d_{exc} = d_{inh} = 0$ ms (cyan square), $d_{exc} = 0$ ms and $d_{inh} = 50$ ms (cyan circle), $d_{exc} = 70$ ms and $d_{inh} = 50$ ms (cyan hexagon), and $d_{exc} = 110$ ms and $d_{inh} = 50$ ms (cyan triangle).

4. DISCUSSION AND CONCLUSION

In this paper, we investigate the influence of delayed conductance on the neuronal synchronization. The study of neuronal synchronization is of great importance in neuroscience, due to the fact that it has been related to cognition, as well as to brain pathology. The conductance between the neurons plays a crucial role in the synchronous behavior. Many studies investigated the
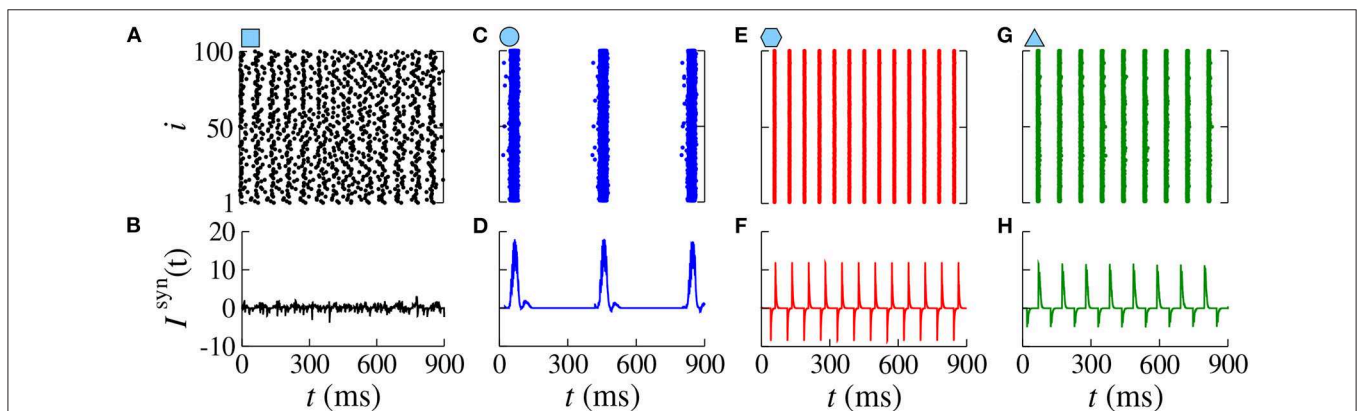

FIGURE 7 | Raster plots (top) and $I^{syn}(t)$ (bottom) for $g_{exc} = 0.8$ nS, $g = 6$ for different values of d_{exc} and d_{inh}. Different delay values generate desynchronized spikes **(A,B)**, synchronized bursts **(C,D)**, synchronized spikes **(E,F)**, and synchronized bursts **(G,H)**.

effects of the conductance on the neuronal activities (Bezanilla, 2008; Kispersky et al., 2012).

We construct a network composed of adaptive exponential integrate-and-fire (AEIF) neurons. The AEIF neuron has been used to mimic spike and burst patterns. In our network, we consider that the neurons are randomly connected by means of inhibitory and excitatory synapses. We find that for some network parameters, it is possible to observe spikes or bursts synchronization. We use the mean order parameter ($\overline{R}$) and the mean coefficient of variation ($\overline{CV}$) as diagnostic tools to identify synchronization and spikes or bursts patterns, respectively. We also calculate $\overline{F}$ and $\overline{I}_s$ to analyse how they are related to synchronous behavior.

In order to explore the effects of different delayed conductances on the neuronal synchronization, in the section 3, we consider delay in both inhibitory and excitatory conductances. When all neurons are spiking (weak coupling), the delays induce synchronization domains in the parameter space $d_{inh} \times d_{exc}$. Inside the parameter domains with synchronized neurons, we observe separated parameter subdomains representing neurons with higher and lower values of the mean firing frequency $\overline{F}$ (Hz), as well as different values of the mean synaptic input $\overline{I}_s$ (pA). For the neuronal network with strong coupling, we do not find domains with behavior similar to weak coupling in the parameter space $d_{inh} \times d_{exc}$. However, we see synchronous and desynchronous activities with either spike and burst activities. We also observe a range of high values of $\overline{F}$ and $\overline{I}_s$ when only inhibitory delayed conductance is increased ($d_{exc} \approx 0$), responsible for turning desynchronous spikes into synchronous burst patterns. For $d_{exc} \approx d_{inh}$ and strong coupling, we also observed desynchronous spike activities. Desynchronous spike activities can be associated with lower mean firing frequency and synaptic currents for strong coupling.

For weak coupling, the size of the region with synchronized behavior in $d_{inh} \times d_{exc}$ decreases when the number of connections is decreased. In this situation, we observe that the size of the small regions can be increased by increasing g_{exc}. In addition, for strong coupling and decreasing the number of connections, there is no burst activity and we verify the existence of synchronized and desynchronized spiking patterns, as shown for weak coupling and no sparse connectivity. Therefore, the connectivity and the synaptic conductance play an important role in the synchronization.

In conclusion, we verify that the delay in the conductances plays a crucial role in the behavior of the neurons in the neuronal network. For weak coupling, we uncover that not only the synchronous behavior, but also the mean firing frequency and the mean synaptic input depend on the delayed inhibitory and excitatory conductances. We identify which range of synaptic current allow the neuronal network to achieve and maintain synchronous activities. In the region with desynchronized activities, excitatory and inhibitory currents arrive in different times, consequently, high synchronization does not appear. For strong coupling, we see that also spike and burst patterns depend on the delayed conductances. The domain with synchronous pattern is characterized by having different delays in the inhibitory and excitatory conductances. Considering $d_{exc} \approx d_{inh}$, we observe desynchronous spikes activities for both weak and strong coupling. In addition, our results demonstrate that not only intensity of synaptic conductance, but also a short delay in the inhibitory conductance are relevant to avoid abnormal neuronal synchronization.

Our results can be useful to clarify how synchronous and desynchronous activities are reached in a context of neuronal population with delayed conductance. In future works, we plan to analyse the influence of the connection probability between excitatory and inhibitory neurons in the neuronal synchronization, as well as the appearance of clusters synchronization.

DATA AVAILABILITY STATEMENT

The raw data supporting the conclusions of this article will be made available by the authors, without undue reservation.

AUTHOR CONTRIBUTIONS

PP, FB, KI, EL, and MH designed the work, developed the theory, and performed the numerical simulations. AB wrote the manuscript with support from MB, IC, JS, and JK. The authors revised the manuscript several times and gave promising suggestions. All authors also contributed to manuscript revision, read, and approved the submitted version.

FUNDING

REFERENCES

Abbott, L. F., and van Vreeswijk, C. (1993). Asynchronous states in networks of pulse-coupled oscillators. *Phys. Rev. E* 48:1483. doi: 10.1103/PhysRevE.48.1483

Aston-Jones, G., Foote, S. L., and Segal, M. (1985). Impulse conduction properties of noradrenergic locus coeruleus axons projecting to monkey cerebrocortex. *Neuroscience* 15, 765–777. doi: 10.1016/0306-4522(85)90077-6

Bartsch, R. P., Liu, K. K. L., Bashan, A., and Ivanov, P. Ch. (2015). Network Physiology: how organ systems dynamically interact. *PLoS ONE* 10:e0142143. doi: 10.1371/journal.pone.0142143

Bashan, A., Bartsch, R. P., Kantelhardt, J. W., Havlin, S., and Ivanov, P. Ch. (2012). Network physiology reveals relations between network topology and physiologic function. *Nat. Commun.* 3, 1–9. doi: 10.1038/ncomms1705

Batista, C. A. S., Lopes, S. R., Viana, R. L., and Batista, A. M. (2010). Delayed feedback control of bursting synchronization in a scale-free neuronal network. *Neural Netw.* 23, 114–124. doi: 10.1016/j.neunet.2009.08.005

Batista, C. A. S., Szezech, J. D. Jr., Batista, A. M., and Macau, E. E. N., Viana, R. L. (2017). Synchronization of phase oscillators with coupling mediated by a diffusing substance. *Phys. A* 470, 236–248. doi: 10.1016/j.physa.2016.11.140

Batista, C. S., Batista, A. M., de Pontes, J. A., Viana, R. L., and Lopes, S. R. (2007). Chaotic phase synchronization in scale-free networks of bursting neurons. *Phys. Rev. E* 76:016218. doi: 10.1103/PhysRevE.76.016218

Bezanilla, F. (2008). Ion channels: from conductance to structure. *Neuron* 60, 456–468. doi: 10.1016/j.neuron.2008.10.035

Borges, F. S., Iarosz, K. C., Ren, H. P., Batista, A. M., Baptista, M. S., Viana, R. L., et al. (2014). Model of tumour growth with treatment by continuous and pulsed chemotherapy. *Biosystems* 116, 43–48. doi: 10.1016/j.biosystems.2013.12.001

Borges, F. S., Lameu, E. L., Iarosz, K. C., Protachevicz, P. R., Caldas, I. L., Viana, R. L., et al. (2018). Inference of topology and the nature of synapses, and the flow of information in neuronal networks. *Phys. Rev. E* 97:022303. doi: 10.1103/PhysRevE.97.022303

Borges, F. S., Protachevicz, P. R., Lameu, E. L., Bonetti, R. C., Iarosz, K. C., Caldas, I. L., et al. (2017b). Synchronised firing patterns in a random network of adaptive exponential integrate-and-fire neuron model. *Neural Netw.* 90, 1–7. doi: 10.1016/j.neunet.2017.03.005

Borges, R. R., Borges, F. S., Lameu, E. L., Batista, A. M., Iarosz, K. C., Caldas, I. L., et al. (2017a). Spike timing-dependent plasticity induces non-trivial topology in the brain. *Neural Netw.* 88, 58–64. doi: 10.1016/j.neunet.2017.01.010

Brette, R., and Gerstner, W. (2005). Adaptive exponential integrate-and-fire model as an effective description of neuronal activity. *J. Neurophysiol.* 94, 3637–3642. doi: 10.1152/jn.00686.2005

Brunel, N. (2000). Dynamics of networks of randomly connected excitatory and inhibitory spiking neurons. *J. Physiol.* 94, 445–463. doi: 10.1016/S0928-4257(00)01084-6

Byrne, H. M. (1997). The effect of time delays on the dynamics of avascular tumor growth. *Math. Biosci.* 144, 83–117. doi: 10.1016/S0025-5564(97)00023-0

Chen, B., Engelbrecht, J. R., and Mirollo, R. (2017). Cluster synchronization in networks of identical oscillators with α-function pulse coupling. *Phys. Rev. E* 95:022207. doi: 10.1103/PhysRevE.95.022207

Chen, Z., Hu, K., Stanley, H. E., Novak, V., and Ivanov, P. Ch. (2006). Cross-Correlation of instantaneous phase increments in pressure-flow fluctuations: applications to cerebral autoregulation. *Phys. Rev. E* 73:031915. doi: 10.1103/PhysRevE.73.031915

Deco, G., Buehlmann, A., Masquelier, T., and Hugues, E. (2011). The role of rhythmic neural synchronization in rest and task conditions. *Front. Hum. Neurosci.* 5:4. doi: 10.3389/fnhum.2011.00004

Deco, G., Jirsa, V., Mcintosh, A. R., Sporns, O., and Kötter, R. (2009). Key role of coupling, delay, and noise in resting brain fluctuations. *Proc. Natl. Acad. Ssi. U.S.A.* 106, 10302–10307. doi: 10.1073/pnas.0901831106

Dhamala, M., Jirsa, V. K., and Ding, M. (2004). Enhancement of neural synchrony by time delay. *Phys. Rev. Lett.* 92:074104. doi: 10.1103/PhysRevLett.92.074104

di Volo, M., Romagnoni, A., Capone, C., and Destexhe, A. (2019). Biologically realistic mean-field models of conductance-based networks of spiking neurons with adaptation. *Neural Comput.* 31, 653–680. doi: 10.1162/neco_a_01173

Ermentrout, G. B., and Kopell, N. (1998). Fine structure of neural spiking and synchronization in the presence of conduction delays. *Proc. Natl. Acad. Ssi. U.S.A.* 95, 1259–1264. doi: 10.1073/pnas.95.3.1259

Esfahani, Z. G., Gollo, L. L., and Valizadeh, A. (2016). Stimulus-dependent synchronization in delayed-coupled neuronal networks. *Sci. Rep.* 6:23471. doi: 10.1038/srep23471

Fardet, T., Ballandras, M., Bottani, S., Métens, S., and Monceau, P. (2018). Understanding the generation of network bursts by adaptive oscillatory neurons. *Front. Neurosci.* 2:41. doi: 10.3389/fnins.2018.00041

Glass, L., Beuter, A., and Larocque, D. (1988). Time delays, oscillations and chaos in physiological control systems. *Math. Biosci.* 90, 111–125. doi: 10.1016/0025-5564(88)90060-0

Hodgkin, A. L., and Huxley, A. F. (1952). A quantitative description of membrane curent and its application to conduction and excitation in nerve. *J. Physiol.* 117, 500–544. doi: 10.1113/jphysiol.1952.sp004764

Ivanov, P. C., Liu, K. K. L., and Bartsch, R. (2016). Focus on the emerging new fields of network physiology and network medicine. *New J. Phys.* 18:100201. doi: 10.1088/1367-2630/18/10/100201

Ivanov, P. C., Ma, Q. D. Y., and Bartsch, R. P. (2009). Maternal-fetal heartbeat phase-synchronization. *Proc. Natl. Acad. Sci. U.S.A.* 106, 13641–13642. doi: 10.1073/pnas.0906987106

Kim, S.-Y., and Lim, W. (2018a). Stochastic spike synchronization in a small-world neural network with spike-timing-dependent plasticity. *Neural Netw.* 97, 92–106. doi: 10.1016/j.neunet.2017.09.016

Kim, S.-Y., and Lim, W. (2018b). Effect of inhibitory spike-timing-dependent plasticity on fast sparsely synchronized rhythms in a small-world neuronal network. *Neural Netw.* 106, 50–66. doi: 10.1016/j.neunet.2018.06.013

Kispersky, T. J., Caplan, J. S., and Marder, E. (2012). Increase in sodium conductance decreases firing rate and gain in model neurons. *J. Neurosci.* 32, 10995–11004. doi: 10.1523/JNEUROSCI.2045-12.2012

Kuramoto, Y. (1984). *Chemical Oscillations, Waves, and Turbulence.* Berlin: Springer-Verlag.

Lapicque, L. (1907). Recherches quantitatives sur l'excitation électrique des nerfs traitée comme une polarisation. *J. Physiol. Pathol. Gen.* 9, 620–635.

Liu, K. K. L., Bartsch, R. P., Lin, A., Mantegna, R. N., and Ivanov, P. Ch. (2015). Plasticity of brain wave network interactions and evolution across physiologic states. *Front. Neural Circuits* 9:62. doi: 10.3389/fncir.2015.00062

Mier-y-Terán-Romero, L., Silber, M., and Hatzimanikatis, V. (2010). The origins of time-delay in template biopolymerization processes. *PLoS Comput. Biol.* 6:e1000726. doi: 10.1371/journal.pcbi.1000726

Naud, R., Marcille, N., Clopath, C., and Gerstner, W. (2008). Firing patterns in the adaptive exponential integrate-and-fire model. *Biol. Cybernet.* 99, 335–347. doi: 10.1007/s00422-008-0264-7

Noback, C. R., Strominger, N. L., Demarest, R. J., and Ruggiero, D. A. (2005). *The Human Nervous System: Structure and Function.* Totowa, NJ: Humana Press.

Olmi, S., Torcini, A., and Politi, A. (2014). Linear stability in networks of pulsed-coupled neurons. *Front. Comput. Neurosci.* 8:8. doi: 10.3389/fncom.2014.00008

Pérez, T., Garcia, G. C., Eguíluz, V. M., Vicente, R., Pipa, G., and Mirasso, C. (2011). Effect of the topology and delayed interactions in neuronal networks synchronization. *PLoS ONE* 6:e19900. doi: 10.1371/journal.pone.0019900

Pikovsky, A. S., Rosenblum, M. G., Osipov, G. V., and Kurths, J. (1997). Phase synchronization of chaotic oscillators by external driving. *Phys. D* 104, 219–238. doi: 10.1016/S0167-2789(96)00301-6

Protachevicz, P. R., Borges, F. S., Lameu, E. L., Ji, P., Iarosz, K. C., Kihara, A. H., et al. (2019). Bistable firing pattern in a neural network model. *Front. Comput. Neurosci.* 13:19. doi: 10.3389/fncom.2019.00019

Protachevicz, P. R., Borges, R. R., Reis, A. S., Borges, F. S., Iarosz, K. C., Caldas, I. L., et al. (2018). Synchronous behaviour in network model based on human cortico-cortical connections. *Physiol. Meas.* 39:074006. doi: 10.1088/1361-6579/aace91

Santos, M. S., Protachevicz, P. R., Iarosz, K. C., Caldas, I. L., Viana, R. L., Borges, F. S., et al. (2019). Spike-burst chimera states in an adaptive exponential integrate-and-fire neuronal network. *Chaos* 29:043106. doi: 10.1063/1.5087129

Stepan, G. (2009). Delay effects in brain dynamics. *Philos. Trans. R. Soc. A* 367, 1059–1062. doi: 10.1098/rsta.2008.0279

Stoelzel, C. R., Bereshpolova, Y., Alonso, J.-M., and Swadlow, H. A. (2017). Axonal conduction delays, brain state, and corticogeniculate communication. *J. Neurosci.* 37, 6342–6358. doi: 10.1523/JNEUROSCI.0444-17.2017

Sun, G.-Q., Wang, S.-L., Ren, Q., Jin, Z., and Wu, Y.-P. (2015). Effects of time delay and space on herbivore dynamics: linking inducible defenses of plants to herbivore outbreak. *Sci. Rep.* 5:11246. doi: 10.1038/srep11246

Tang, J., Ma, J., Yi, M., Xia, H., and Yang, X. (2011). Delay and diversity-induced synchronization transitions in a small-world neuronal network. *Phys. Rev. E* 83:046207. doi: 10.1103/PhysRevE.83.046207

Uhlhaas, P. J., and Singer, W. (2006). Neural synchrony in brain disorders: relevance for cognitive dysfunctions and pathophysiology. *Neuron* 52, 155–168. doi: 10.1016/j.neuron.2006.09.020

van Vreeswijk, C. (1996). Partial synchronization in populations of pulse-coupled oscillators. *Phys. Rev. E* 54:5522. doi: 10.1103/PhysRevE.54.5522

van Vreeswijk, C., Abbott, L. F., and Ermentrout, G. B. (1994). When not excitation synchronizes neural firing. *J. Comput. Neurosci.* 1, 313–321. doi: 10.1007/BF00961879

Wang, L., Zhao, H., and Cao, J. (2016). Synchronized bifurcation and stability in a ring of diffusively coupled neurons with time delay. *Neural Netw.* 75, 32–46. doi: 10.1016/j.neunet.2015.11.012

Xu, L., Chen, Z., Hu, K.un, Stanley, H. E., and Ivanov, P. Ch. (2006). Spurious detection of phase synchronization in coupled nonlinear oscillators. *Phys. Rev. E* 73:065201. doi: 10.1103/PhysRevE.73.065201